European Radiology (2019) 29:6477–6488
https://doi.org/10.1007/s00330-019-06331-4

GASTROINTESTINAL

Prospective comparison of transient, point shear wave, and magnetic resonance elastography for staging liver fibrosis

Thierry Lefebvre[1,2,3] · Claire Wartelle-Bladou[4] · Philip Wong[5] · Giada Sebastiani[5] · Jeanne-Marie Giard[2,4] · Hélène Castel[2,4] · Jessica Murphy-Lavallée[1] · Damien Olivié[1] · André Ilinca[1,2] · Marie-Pierre Sylvestre[2,6] · Guillaume Gilbert[1,7] · Zu-Hua Gao[8] · Bich N. Nguyen[9] · Guy Cloutier[1,10,11] · An Tang[1,2,10]

Received: 1 February 2019 / Revised: 16 May 2019 / Accepted: 13 June 2019 / Published online: 5 July 2019

Abstract

Objectives To perform head-to-head comparisons of the feasibility and diagnostic performance of transient elastography (TE), point shear-wave elastography (pSWE), and magnetic resonance elastography (MRE).

Methods This prospective, cross-sectional, dual-center imaging study included 100 patients with known or suspected chronic liver disease caused by hepatitis B or C virus, nonalcoholic fatty liver disease, or autoimmune hepatitis identified between 2014 and 2018. Liver stiffness measured with the three elastographic techniques was obtained within 6 weeks of a liver biopsy. Confounding effects of inflammation and steatosis on association between fibrosis and liver stiffness were assessed. Obuchowski scores and AUCs for staging fibrosis were evaluated and the latter were compared using the DeLong method.

Results TE, pSWE, and MRE were technically feasible and reliable in 92%, 79%, and 91% subjects, respectively. At univariate analysis, liver stiffness measured by all techniques increased with fibrosis stages and inflammation and decreased with steatosis. For classification of dichotomized fibrosis stages, the AUCs were significantly higher for distinguishing stages F0 vs. ≥ F1 with MRE than with TE (0.88 vs. 0.71; $p < 0.05$) or pSWE (0.88 vs. 0.73; $p < 0.05$), and for distinguishing stages ≤ F1 vs. ≥ F2 with MRE than with TE (0.85 vs. 0.75; $p < 0.05$). TE, pSWE, and MRE Obuchowski scores for staging fibrosis stages were respectively 0.89 (95% CI 0.85–0.93), 0.90 (95% CI 0.85–0.94), and 0.94 (95% CI 0.91–0.96).

Conclusion MRE provided a higher diagnostic performance than TE and pSWE for staging early stages of liver fibrosis.

Trial registration NCT02044523

Electronic supplementary material The online version of this article (https://doi.org/10.1007/s00330-019-06331-4) contains supplementary material, which is available to authorized users.

✉ An Tang
an.tang@umontreal.ca

[1] Department of Radiology, Radio-Oncology and Nuclear Medicine, Université de Montréal, Montreal, Canada

[2] Centre de recherche du Centre hospitalier de l'Université de Montréal (CRCHUM), Montreal, Canada

[3] Medical Physics Unit, McGill University, Montreal, Canada

[4] Department of Medicine, Division of Hepatology and Liver Transplantation, Université de Montréal, Montreal, Canada

[5] Department of Medicine, Division of Gastroenterology and Hepatology, McGill University Health Centre (MUHC), Montreal, Canada

[6] Department of Social and Preventive Medicine, École de santé publique de l'Université de Montréal (ESPUM), Montreal, Canada

[7] MR Clinical Science, Philips Healthcare Canada, Markham, Canada

[8] Department of Pathology, McGill University, Montreal, Canada

[9] Service of Pathology, Centre hospitalier de l'Université de Montréal (CHUM), Montreal, Canada

[10] Institute of Biomedical Engineering, Université de Montréal, Montreal, Canada

[11] Laboratory of Biorheology and Medical Ultrasonics (LBUM), Centre de recherche du Centre hospitalier de l'Université de Montréal (CRCHUM), Montreal, Canada

Key Points

- *The technical failure rate was similar between MRE and US-based elastography techniques.*
- *Liver stiffness measured by MRE and US-based elastography techniques increased with fibrosis stages and inflammation and decreased with steatosis.*
- *MRE provided a diagnostic accuracy higher than US-based elastography techniques for staging of early stages of histology-determined liver fibrosis.*

Keywords Fibrosis · Liver · Classification · Elasticity imaging techniques · Prospective studies

Abbreviations

AIH	Autoimmune hepatitis
AUC	Area under the receiver operating characteristic curve
CLD	Chronic liver disease
HBV	Hepatitis B virus
HCV	Hepatitis C virus
MRE	Magnetic resonance elastography
NAFLD	Nonalcoholic fatty liver disease
NASH	Nonalcoholic steatohepatitis
pSWE	Point shear wave elastography
TE	Transient elastography

Introduction

In patient care, staging of liver fibrosis has important implications for disease prognosis and management decisions. The reference standard remains liver biopsy to assess the severity of liver fibrosis, the grade of steatosis, and the inflammatory activity, and to determine which patients might benefit from pharmacological therapy [1]. However, limitations of liver biopsy have been highlighted in recent years [2]. In response to these shortcomings, alternate noninvasive methods have been developed to detect liver fibrosis in patients with chronic liver disease (CLD) [3]. Among these noninvasive techniques, elastography is generally considered to provide the highest diagnostic performance for staging fibrosis [4, 5].

Elastography methods measure mechanical properties, namely stiffness quantified using the elasticity modulus or acoustic shear wave propagation speed, which represents a surrogate biomarker of liver fibrosis. These techniques rely on the concept that stiffness tends to be low in normal liver and increases with fibrotic liver. Clinically available elastography techniques include transient elastography (TE), point shear wave elastography (pSWE), and MR elastography (MRE). Although meta-analyses have reported a higher diagnostic accuracy for MRE compared with that for US-based elastography techniques [5–7], these comparisons are prone to selection biases due to different eligibility criteria, patient populations, and referral patterns. Hence, there is a need to perform paired comparisons of the most commonly used elastography techniques in the same patient population.

The purpose of this study was to perform a head-to-head comparison of the feasibility and diagnostic performance of TE, pSWE, and MRE for detecting histology-determined fibrosis in patients with CLD. The secondary objective was to evaluate the influence of potential confounders (i.e., inflammation and steatosis) on association between fibrosis and stiffness measurements.

Materials and methods

Study design and subjects

This cross-sectional imaging trial was approved by the Institutional Review Board of the two participating institutions, Centre hospitalier de l'Université de Montréal and McGill University Health Centre (ClinicalTrials.gov Identifier No. NCT02044523). All subjects provided written informed consent. TE, pSWE, and MRE examinations were performed as research procedures within 6 weeks of the liver biopsy for all patients, and if done after the liver biopsy, a minimum delay of 48 h was observed. Histopathology was used as the reference standard. Feasibility and fibrosis-staging accuracy of the three index tests were compared.

The hepatology clinics of the two participating institutions recruited consecutive patients between January 2014 and September 2018. Adult participants were enrolled in this study if (a) they underwent a liver biopsy as part of their clinical standard of care for suspected or known chronic liver disease caused by hepatitis B virus (HBV) infection, hepatitis C virus (HCV) infection, nonalcoholic fatty liver disease (NAFLD), nonalcoholic steatohepatitis (NASH), or autoimmune hepatitis (AIH); or (b) they underwent a liver biopsy to resolve an unexplained discrepancy between the fibrosis stages inferred by TE results and by noninvasive scoring systems based on laboratory tests. Participants were excluded if they had any contraindication to MRI.

TE examination

TE using the FibroScan (Echosens) was used to measure the median Young elasticity modulus (in kPa) as a surrogate of

liver fibrosis. The M probe was used by default. The XL probe was used in case of high BMI or failure to measure the liver stiffness with the M probe [8]. Experienced hepatologists or nurses positioned the transducer on the skin at an intercostal space over the right liver lobe. At this site, TE was repeated up to 20 times, until at least 10 valid measurements were collected. Failure was defined as the impossibility of obtaining 10 valid measurements [9]. Reliability was defined according to the clinically used criteria proposed by Boursier et al based on the ratio of the interquartile range to the median (IQR/M) [9].

pSWE examination

Conventional ultrasound images in B-mode and acoustic radiation force impulse imaging (ACUSON S2000 or S3000, Siemens Healthineers) were acquired with the same convex probe (4C1, Siemens Healthineers), tissue harmonic imaging (4 MHz), and a mechanical index of 1.7. pSWE examination was performed according to the clinical guidelines by experienced hepatologists or nurses [10]. The median shear wave velocity (in m/s) was considered representative of liver stiffness, and the IQR/M was used as an indicator of variability. Technical success was achieved if 10 valid measurements were obtained in 20 repetitions or less. Reliability was defined according to clinical guidelines using the success rate and the IQR/M [10].

MRE examination

All MR examinations were performed on a 3.0-T clinical scanner (Achieva TX; Philips Healthcare) in accordance with a previously described method [11]. A transducer (Resoundant) positioned on the right side of the patient in supine position induced a mechanical vibration at 60 Hz synchronized with the acquisition of a motion-sensitized gradient-echo (GRE) sequence. The MRE image analysis technique included elastogram images with parametric maps of goodness-of-fit to exclude areas of unreliable measurements from the region of interest (ROI). Further details of MR acquisition and post-processing parameters to compute the shear modulus (in kPa) are provided in the Supplemental Materials. Measures of iron (R2*) were performed. MRE measurements were considered reliable if R2* was in the normal range (lower than 126 s^{-1} at 3.0 T) [12, 13].

Histopathological analysis

Liver biopsies were performed with 16-G or 18-G core needles according to the clinical standard of care. Hematoxylin and eosin (H&E) slides were centrally scored by an expert liver pathologist. Fibrosis stages, inflammation grades, and steatosis grades were assessed. Details of fibrosis scoring are provided in the Supplemental Materials.

Blinding

Technologists, sonographers, physicians, and image analysts participating in the analysis of the index tests were blinded to histopathological results. The pathologist was blinded to elastography results.

Statistical analysis

Statistical analyses were performed by a senior-level biostatistician with the SAS 9.4 (SAS Institute) and the free software R3.4.2 (R Foundation).

Feasibility and reliability The technical feasibility and reliability rates were calculated. Pairwise comparisons of the rates were performed using the McNemar test reflecting the fact that index tests were performed on the same

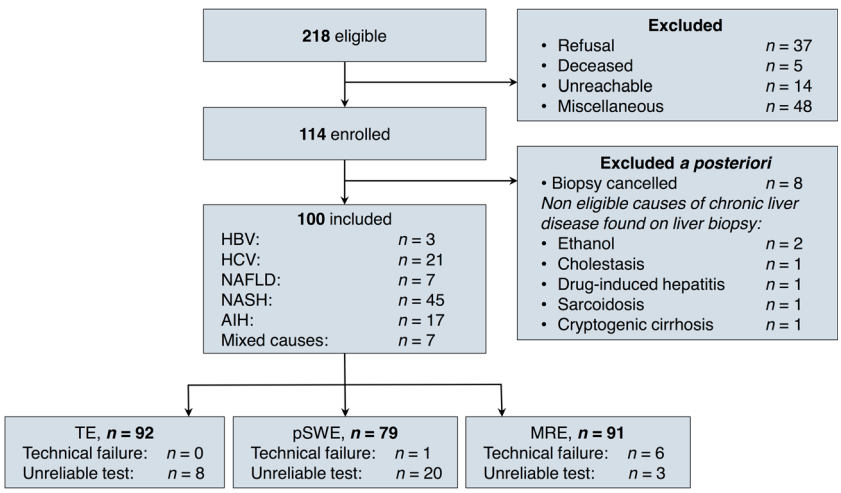

Fig. 1 Flowchart of patient selection

Table 1 Characteristics in 100 patients

Characteristic	Data
Sex	
Male	53 (53%)
Female	47 (47%)
Age (years)	
Mean ± SD (range)	55 ± 12 (22–78)
BMI (kg/m^2)	
Mean ± SD (range)	30.1 ± 5.9 (17–47)
< 25	20 (20%)
≥ 25 and < 30	27 (27%)
≥ 30 and < 40	48 (48%)
≥ 40	5 (5%)
Racial category	
White	74 (74%)
Black	6 (6%)
Asian	5 (5%)
American Indian	2 (2%)
Hawaiian or Pacific Islander	1 (1%)
N/A	12 (12%)
Ethnic category	
Hispanic/Latino	6 (6%)
Non-Hispanic	94 (94%)
Diabetes	30 (30%)
Hypertension	37 (37%)
Laboratory tests: mean ± SD (range)	
AST (U/L)	53 ± 47 (14–319)
ALT (U/L)	76 ± 78 (13–473)
GGT (U/L)	98 ± 205 (10–1586)
Platelet count (× 10^9/L)	201 ± 65 (78–383)
Total bilirubin (μmol/L)	13.98 ± 8.71 (5–73)
Prothrombin time (%)	100.1 ± 8.2 (80–120)
Alkaline phosphatase (U/L)	74 ± 36 (29–217)
Albumin (g/L)	40.43 ± 5.92 (31–79)
Cholesterol (mmol/L)	4.56 ± 1.04 (2.9–7.6)
Biopsy length (mm)	
Mean ± SD (range)	20.5 ± 5.2 (10–30)
Fibrosis stage	
F0 (none)	15 (15%)
F1 (perisinusoidal or periportal)	16 (16%)
F2 (periportal and presence of septa)	24 (24%)
F3 (numerous septa without cirrhosis)	18 (18%)
F4 (cirrhosis)	27 (27%)
Inflammation activity grade	
A0 (none)	9 (9%)
A1 (negligible)	49 (49%)
A2 (moderate)	32 (32%)
A3 (severe)	10 (10%)
Steatosis grade	
S0 (< 5% hepatocytes involved)	35 (35%)
S1 (5–33% hepatocytes involved)	27 (27%)
S2 (33–66% hepatocytes involved)	18 (18%)
S3 (> 66% hepatocytes involved)	20 (20%)
Iron	
0	71 (71%)
1	16 (16%)
2	4 (4%)
3	0 (0%)
4	0 (0%)
N/A	9 (9%)

Numbers in parentheses are percentages, unless otherwise specified

SD standard deviation, *BMI* body mass index, *AST* aspartate aminotransferase, *ALT* alanine aminotransferase, *GGT* gamma-glutamyl transpeptidase

subjects. Technically unfeasible or unreliable measurements were excluded from further analyses.

Staging comparison Comparison of index tests' measurements between all fibrosis stages was performed using the nonparametric Kruskal-Wallis rank-sum test with Bonferroni's correction. Pairwise comparisons were performed between fibrosis stages with a post hoc Mann-Whitney *U* test in each index test.

Diagnostic performance The diagnostic accuracy of stiffness measurements by TE, pSWE, and MRE for predicting histology-determined fibrosis stage was assessed by the Obuchowski score, a multinomial version of the area under the receiver operating characteristic (ROC) curve [14], and the area under the ROC curve (AUC). Estimates of diagnostic performance (including sensitivity, specificity, accuracy, positive predictive value, and negative predictive value) were calculated for the threshold that provided at least 90% sensitivity for differentiation of F0 vs. ≥ F1, ≤ F1 vs. ≥ F2, ≤ F2 vs. ≥ F3, and ≤ F3 vs. F4. Measures of AUC of TE, pSWE, and MRE were compared using the DeLong method.

Confounding variables Spearman's rank correlation and multiple regression analysis of TE, pSWE, and MRE measurements as a function of fibrosis, inflammation, and steatosis were performed to evaluate the confounding effect of these histological features on liver stiffness. Spearman's ρ, regression coefficient estimates, normalized regression coefficient estimates, standard deviation, and adjusted R^2 were reported for each technique.

Table 2 TE, pSWE, and MRE mean values as a function of fibrosis stage

Technique	F0	F1	F2	F3	F4	*p* value
Young's modulus, TE (kPa)	8.0 ± 3.0	8.2 ± 2.7	9.0 ± 3.1	11.1 ± 4.1	22.0 ± 15.6	< 0.0001
Shear wave speed, pSWE (m/s)	1.22 ± 0.65	1.22 ± 0.66	1.25 ± 0.17	1.46 ± 0.33	2.16 ± 0.74	< 0.0001
Shear modulus, MRE (kPa)	2.11 ± 0.27	2.46 ± 0.47	2.65 ± 0.54	3.32 ± 0.92	4.40 ± 1.40	< 0.0001

TE transient elastography, *pSWE* point shear wave elastography, *MRE* magnetic resonance elastography

Results

Population

Our cohort included 100 eligible adult patients who underwent TE, pSWE, MRE, and liver biopsy between January 2014 and July 2018 (Fig. 1). Seventy-nine patients were recruited at Centre hospitalier de l'Université de Montréal and 21 at McGill University Health Centre. Mean age was 55 years (22–78) (Table 1). Forty-seven were women (47%), and all patients had suspected or known liver fibrosis or cirrhosis induced by either HBV ($n = 3$), HCV ($n = 21$), NAFLD ($n = 7$), NASH ($n = 45$), AIH ($n = 17$), or mixed causes ($n = 7$). Histopathological findings had the following distribution in our study cohort: for fibrosis stage, 15 patients had F0, 16 F1, 24 F2, 18 F3, and 27 F4; for inflammation activity grade, 9 patients had A0, 49 A1, 32 A2, and 10 A3; for steatosis grade, 35 patients had grade S0, 27 grade S1, 18 grade S2, and 20 grade S3. Some patients were overweight ($n = 27$), obese ($n = 48$), or severely obese ($n = 5$). The mean body mass index (BMI) of the cohort was 30.1 ± 5.9 kg/m^2. The median time interval between TE, pSWE, and MRE and liver biopsy was 5 days (0–31 days), 11 days (0–31 days), and 11 days (0–31 days), respectively. Average H&E slide length was 20.5 mm (10–30 mm) and included 2 fragments on average (1–13). Fifty-eight TE examinations were performed with the M probe and 42 with the XL probe.

Feasibility and reliability

The technical failure rate was 0% for TE, 1% for pSWE, and 6% for MRE. Technical failure rate differences were not significant between all the elastographic techniques. The rate of unreliable examinations was 8% for TE, 19% for pSWE, and 3% for MRE. Reliability differences were significant only between TE and pSWE ($p < 0.05$) and between pSWE and MRE ($p < 0.001$). For MR examinations, mean R2* was 50.6 ± 16.5 s^{-1} (13.1–112.8 s^{-1}) in the population with measurements deemed reliable ($n = 91$) and 147.4 ± 39.8 s^{-1} (127.4–220.0 s^{-1}) in the population with measurements deemed unreliable ($n = 3$).

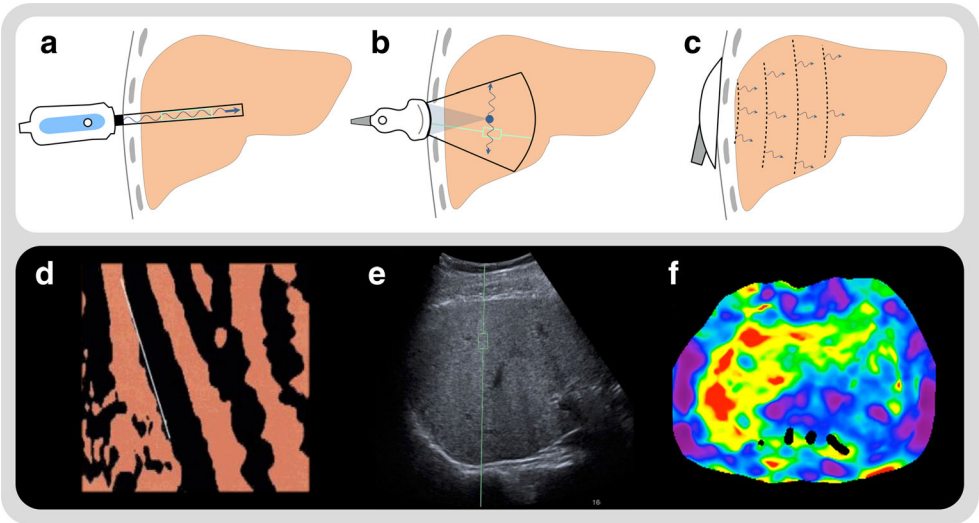

Fig. 2 Schematic diagrams of (**a**) TE, (**b**) pSWE, and (**c**) MRE liver stiffness measurements. **d** TE stiffness measurement, (**e**) pSWE stiffness measurement, and (**f**) MRE elastogram in a cirrhotic obese male patient with hepatitis C virus, BMI = 30.8 kg/m^2. Liver stiffness: TE Young's modulus = 20.90 kPa; pSWE shear wave speed = 1.75 m/s; and MRE shear modulus = 5.48 kPa. Liver biopsy: percutaneous biopsy; sample length = 22 mm; fibrosis stage = F0; inflammation activity grade = A3; and steatosis grade = S3

Stiffness measurements

Mean stiffness measurements with standard deviations for each fibrosis stage in all techniques are reported in Table 2. Examples of TE, pSWE, and MRE measurements are shown in Fig. 2, and boxplots are shown in Fig. 3.

Staging comparison

Stiffness measurements with TE, pSWE, and MRE differed significantly between histology-determined fibrosis stages ($p < 0.0001$). Post hoc tests revealed that stiffness measurements differed significantly between ≤ F1 vs. ≥ F2 for pSWE ($p < 0.05$), ≤ F2 vs. ≥ F3 for MRE ($p < 0.05$), and ≤ F3 vs. F4 for all techniques ($p < 0.001$, $p < 0.05$, and $p < 0.05$, respectively).

Diagnostic performance

Estimates of diagnostic performance are shown in Table 3 and ROC analysis in Fig. 4. AUCs were similar or higher for detecting any dichotomized fibrosis stages with MRE than with TE or pSWE. For differentiating F0 vs. ≥ F1, the AUC was significantly higher for MRE than that for TE (0.88 vs. 0.71; $p < 0.05$) or pSWE (0.88 vs. 0.73; $p < 0.05$). For differentiating ≤ F1 vs. ≥ F2, the AUC was significantly higher for MRE than that for TE (0.85 vs. 0.75; $p < 0.05$). For differentiating ≤ F2 vs. ≥ F3 and ≤ F3 vs. F4, there were no significant differences in AUCs between the elastographic techniques. Also, there were no significant differences between the AUCs of TE and pSWE for differentiation of fibrosis stages.

Confounding variables

Spearman's rank correlation and multiple regression analysis of the confounding effects of fibrosis, inflammation, and fibrosis on elastographic measurements are shown in Table 4. Scatter plots with linear regression of stiffness measurements with inflammation and steatosis are shown in Figs. 5 and 6, respectively. Univariate correlation coefficients demonstrated that liver stiffness measured with TE, pSWE, and MRE increased significantly with fibrosis stage (0.57 [$p < 0.001$], 0.62 [$p < 0.0001$], and 0.72 [$p < 0.0001$], respectively), increased significantly with inflammation grade (0.20 [$p < 0.05$], 0.23 [$p < 0.05$], and 0.21 [$p < 0.05$], respectively), and decreased with steatosis stage (− 0.11 [$p = 0.14$], − 0.23 [$p < 0.05$], and − 0.22 [$p < 0.05$], respectively). However, multiple regression coefficient estimates demonstrated that liver stiffness measured with TE, pSWE, and MRE increased significantly with fibrosis stage (3.07 [$p < 0.0001$], 0.24 [$p < 0.0001$], and 0.55 [$p < 0.0001$], respectively), but not significantly increased with inflammation grade (0.65 [$p = 0.56$], 0.08 [$p = 0.41$], and 0.13 [$p = 0.32$], respectively), nor significantly decreased with steatosis stage except when measured with pSWE (− 0.05 [$p = 0.94$], − 0.13 [$p < 0.05$], and 0.08 [$p = 0.35$], respectively).

Discussion

In this cohort, the technical failure rates were not significantly different between elastography techniques. At univariate analysis, liver stiffness measured by all techniques increased with fibrosis stages and inflammation and decreased with steatosis. In multiple regression analysis, only fibrosis significantly correlated with stiffness measurements across all techniques, except pSWE which also correlated with steatosis. Diagnostic accuracy for distinguishing early stages of fibrosis was higher with MRE than with TE or pSWE.

Higher rates of unreliable examinations were observed for pSWE than for TE or MRE. The technical failure rates of elastography techniques were lower than previously reported for TE [15], similar or higher to previously reported for pSWE [16–18], and lower than that reported for MRE [19–21].

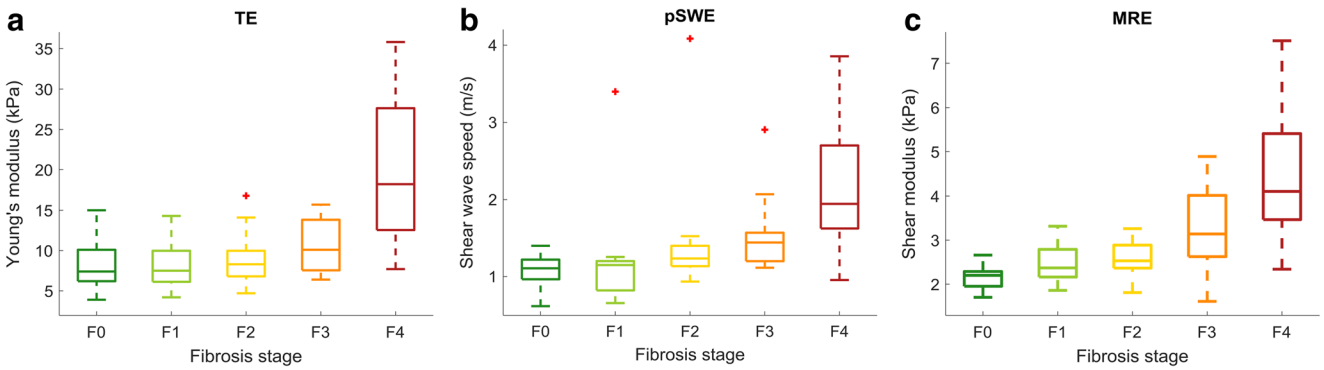

Fig. 3 Median liver stiffness with interquartile ranges measured with index tests vs. histology-determined fibrosis stages. **a** Young's modulus measured with TE. **b** Shear wave speed measured with pSWE. **c** Shear modulus measured with MRE. Stiffness properties with each index test were significantly different between fibrosis stages ($p < 0.0001$). The band inside the box indicates the median, the box indicates the first and third quartiles, whiskers indicate the minimum and maximum values, and red crosses (+) indicate outliers

Table 3 Diagnostic accuracy of Young's modulus by TE, shear wave speed by pSWE, and shear modulus measured by MRE for staging liver fibrosis (95% CI in parenthesis)

Technique	Fibrosis stage	Obuchowski	AUC	Threshold	Sensitivity (%)	Specificity (%)	Accuracy (%)	PPV (%)	NPV (%)
TE	F0 (n = 14) vs. ≥ F1 (n = 78)	0.89 (0.85–0.93)	0.71 (0.59–0.84)	6.1 kPa	89 (80–95)	25 (7–52)	79 (69–86)	86 (77–92)	31 (10–61)
	≤ F1 (n = 29) vs. ≥ F2 (n = 63)		0.75 (0.65–0.85)	6.9 kPa	87 (76–94)	39 (22–58)	71 (62–80)	75 (64–84)	57 (34–78)
	≤ F2 (n = 50) vs. ≥ F3 (n = 42)		0.81 (0.72–0.90)	7.5 kPa	89 (76–96)	45 (32–60)	65 (55–75)	58 (46–70)	83 (64–94)
	≤ F3 (n = 67) vs. F4 (n = 25)		0.85 (0.76–0.95)	8.1 kPa	89 (71–98)	51 (39–63)	61 (51–71)	41 (28–54)	92 (79–98)
pSWE	F0 (n = 11) vs. ≥ F1 (n = 69)	0.90 (0.85–0.94)	0.73 (0.59–0.86)	1.04 m/s	88 (79–94)	25 (6–57)	79 (69–87)	88 (78–94)	25 (6–57)
	≤ F1 (n = 25) vs. ≥ F2 (n = 55)		0.80 (0.71–0.90)	1.12 m/s	90 (80–96)	44 (24–65)	76 (66–85)	79 (68–88)	65 (38–86)
	≤ F2 (n = 42) vs. ≥ F3 (n = 38)		0.82 (0.72–0.91)	1.20 m/s	88 (94–95)	50 (35–65)	68 (57–78)	62 (48–75)	82 (62–94)
	≤ F3 (n = 57) vs. F4 (n = 23)		0.82 (0.71–0.92)	1.21 m/s	88 (70–98)	48 (34–61)	60 (49–70)	43 (29–57)	90 (74–98)
MRE	F0 (n = 13) vs. ≥ F1 (n = 78)	0.94 (0.91–0.96)	0.88 (0.81–0.95)	2.18 kPa	89 (80–95)	43 (18–71)	82 (73–89)	90 (82–96)	40 (16–68)
	≤ F1 (n = 28) vs. ≥ F2 (n = 63)		0.85 (0.77–0.92)	2.23 kPa	90 (80–96)	48 (30–67)	77 (67–85)	80 (70–88)	67 (43–85)
	≤ F2 (n = 51) vs. ≥ F3 (n = 40)		0.88 (0.80–0.95)	2.63 kPa	88 (75–96)	70 (56–82)	78 (69–86)	70 (56–82)	88 (74–96)
	≤ F3 (n = 67) vs. F4 (n = 24)		0.88 (0.79–0.97)	2.75 kPa	89 (70–98)	63 (51–74)	70 (60–79)	47 (33–62)	94 (83–99)

Data in parentheses are raw. *TE* transient elastography, *pSWE* point shear wave elastography, *MRE* magnetic resonance elastography, *AUC* area under the ROC curve, *PPV* positive predictive value, *NPV* negative predictive value

Reliability assessed with similar criteria was found to be similar or higher than that reported for TE [15, 22], lower to previously reported for pSWE [22], and higher than that reported for MRE [19].

As anticipated, stiffness measurements increased with higher fibrosis stages regardless of the technique used [23]. All elastography techniques had a higher accuracy for differentiating fibrosis stages ≤ F3 vs. F4, than for ≤ F2 vs. ≥ F3. This is consistent with prior meta-analyses that have shown higher AUCs for differentiation of higher fibrosis stages [5, 7]. Of note, the accuracy obtained in our study using MRE (0.88) for differentiating F0 from F1 and higher was improved compared with that in previous literature.

Overall, MRE provided either a similar or higher accuracy than TE and pSWE for staging liver fibrosis. The accuracy of MRE was significantly higher than that of TE or pSWE for differentiating F0 from F1 or higher, and significantly higher than that of TE for differentiating F1 or lower from F2 or higher. The MRE technique produces shear waves distributed throughout the liver and includes larger ROIs on four acquired slices whereas pSWE and TE samples include smaller regions of interest (with lengths of 10 mm and 40 mm, respectively).

In prior meta-analyses, higher diagnostic accuracies have been reported for MRE [24] than for pSWE [25] or TE [7]. However, these studies were performed in different patient populations. Hence, there was a need to compare their diagnostic accuracy head-to-head in the same patient population. Some prior studies have performed paired comparisons of diagnostic accuracy between two of the three elastography techniques. A prior study by Cui et al has reported a higher fibrosis-staging accuracy for MRE than for pSWE in patients with NAFLD [26]. Similarly, prior studies comparing the diagnostic performance of MRE and TE have found a higher accuracy for MRE than for TE in patients with CLD [27], chronic HBV [7], or NAFLD [28]. A study by Bohte et al reported a similar diagnostic accuracy for MRE and TE in patients with HBV and HCV [29]. Most studies comparing US-based elastography techniques have found a similar diagnostic accuracy between pSWE and TE in patients with CLD [30], NAFLD [22], and viral hepatitis [31]. One cross-sectional study by Rizzo has found that pSWE was more accurate than TE for the detection of significant fibrosis ≥ F2, severe fibrosis ≥ F3, and cirrhosis F4 [32].

In univariate analysis, we found that liver shear stiffness measured with TE, pSWE, and MRE increased with fibrosis, increased to a lesser degree with inflammation, and decreased with steatosis. These findings were consistent across all the elastography techniques. Inflammation, often accompanied by hepatocyte ballooning and edema, may increase liver stiffness by increased cellularity, cell size, or hydrostatic pressure [33]. The increase in liver stiffness observed with higher inflammation grades is consistent with prior findings in animal studies [34, 35] and in patients with CLD [19, 36, 37]. In a cohort of patients with

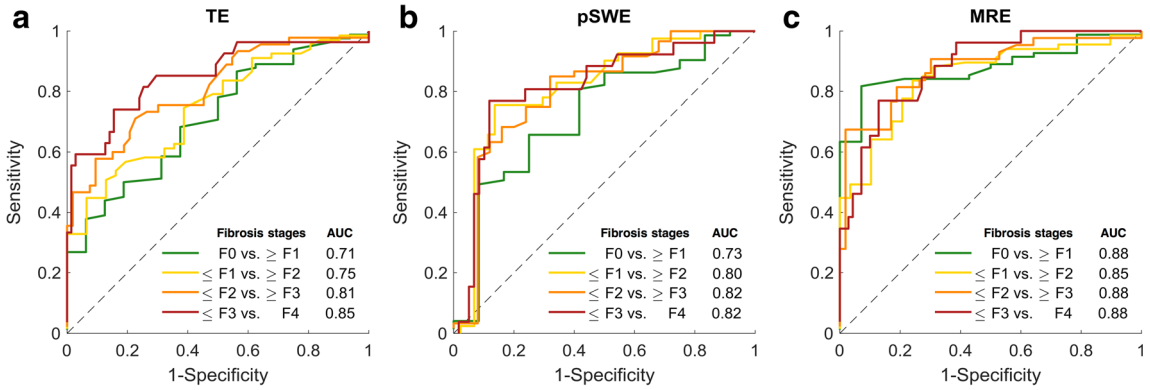

Fig. 4 Receiver operating characteristic curves for distinguishing dichotomized fibrosis stages with (**a**) TE, (**b**) pSWE, and (**c**) MRE. AUCs were similar or higher for detecting any dichotomized fibrosis stages with MRE than with TE or pSWE

HBV, Shi et al obtained similar results for MRE measurements and argued that advanced inflammatory activity (≥ A2) induced higher stiffness measurements especially in lower fibrosis stages (≤ F2) [38].

The impact of steatosis on liver stiffness remains controversial and may depend on the elastography technique used: while some studies have found that steatosis decreases stiffness [39], others have found the opposite [40, 41], and some have found no significant influence [42, 43]. Frequency-dependent viscosity of fat and the use of lower frequencies by TE (50 Hz) and MRE (60 Hz) compared with those used by pSWE (range of 100 to 500 Hz) may explain these discrepancies [44]. Future cross-sectional prospective studies would require quantifying the shear loss modulus (viscosity) to confirm the impact of this confounder. Our results are coherent with those of Yoneda et al who reported a negative correlation of pSWE stiffness measurements with steatosis. When only considering cases with NAFLD of NASH in which fibrosis and steatosis coexist, multivariate analyses also found that steatosis remained a significant confounder only for pSWE. Considering the coexistence of several histopathological changes and the emergence of quantitative techniques for the detection of inflammation using MRE [34], and of fat using MR imaging [45, 46] or ultrasound-based attenuation [47, 48], future multiparametric techniques could improve fibrosis-staging accuracy.

We acknowledge the following limitations. Our study included patients with a variety of CLD, whereas recent studies tend to select homogeneous patient populations with a single etiology. However, our inclusion criteria reflect clinical reality because patients with suspected or multiple coexisting causes of CLD may still require fibrosis staging by noninvasive techniques. Diagnostic accuracy of elastography techniques was lower than previously reported in meta-analyses [17, 24, 49]. The evolution of clinical practice over time has introduced a selection bias toward challenging cases. Nowadays, unambiguous cases are often not biopsied, whereas cases with unreliable elastography results or discrepancies between elastography techniques and blood markers or biological scoring indexes are more likely to undergo liver biopsy. These difficult cases reflect underlying heterogeneity of fibrosis distribution possibly contributing to a lesser diagnostic performance of elastography techniques. Finally, we did not perform colocalization of the ROI sampled

Table 4 Univariate analysis and multiple regression analysis of liver fibrosis, inflammation, and steatosis impact on stiffness measured by index tests

		Univariate analysis		Multiple regression analysis				
		Spearman's ρ	p value	Estimated coefficients	Standardized estimated coefficients	Standard error	p value	Adjusted R^2 value
TE	Fibrosis	0.57	< 0.0001	3.07	0.50	0.62	< 0.0001	0.25
	Inflammation	0.20	< 0.05	0.65	0.06	1.11	0.56	
	Steatosis	− 0.11	0.14	− 0.05	− 0.01	0.73	0.94	
pSWE	Fibrosis	0.62	< 0.0001	0.24	0.46	0.05	< 0.0001	0.29
	Inflammation	0.23	< 0.05	0.08	0.09	0.09	0.41	
	Steatosis	− 0.23	< 0.05	− 0.13	− 0.20	0.07	< 0.05	
MRE	Fibrosis	0.72	< 0.0001	0.55	0.62	0.08	< 0.0001	0.44
	Inflammation	0.21	< 0.05	0.13	0.09	0.13	0.32	
	Steatosis	− 0.22	< 0.05	− 0.08	− 0.08	0.09	0.35	

TE transient elastography, *pSWE* point shear wave elastography, *MRE* magnetic resonance elastography

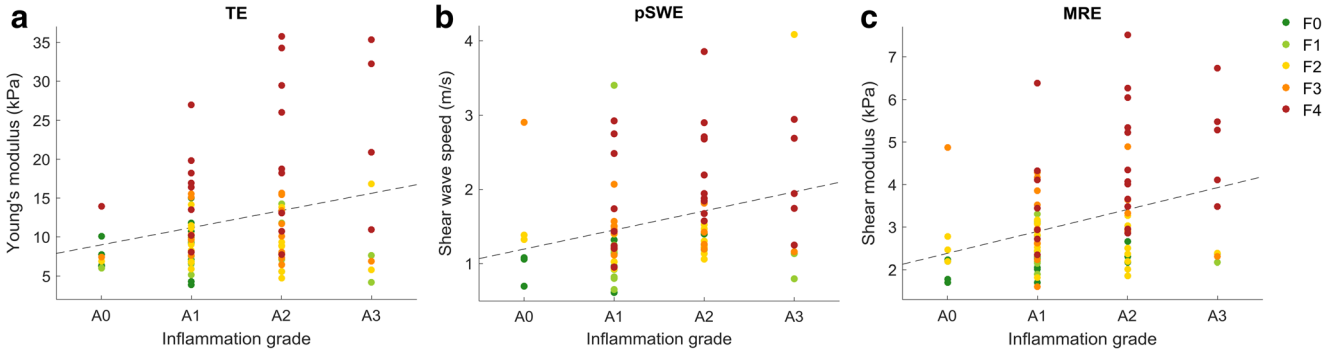

Fig. 5 Scatter plots of stiffness measurements compared with inflammation grades with (**a**) TE, (**b**) pSWE, and (**c**) MRE. Spearman's rho were respectively $\rho = 0.20$, $\rho = 0.23$, and $\rho = 0.21$ ($p < 0.05$ for all)

by the three elastography techniques and intra- and interobserver variability was not evaluated. As shear wave velocities are different in machines from different vendors in ultrasound elastography [50], provided cutoffs might not be applicable to other machines. Instead, we performed elastography examinations according to clinical standards of care by operators blinded to each other and to the reference standard. For TE and pSWE, 10 valid measurements were obtained, and IQR/M was used as a surrogate of variability.

Even though MRE at 3.0 T has been shown to be feasible [51, 52], higher failure rates compared with those for MRE at 1.5 T have been reported especially when using a GRE sequence [20]. MRE using a GRE sequence has higher failure rates than MRE using a spin-echo sequence due to its susceptibility sensitivity [21, 53]. At our center, light iron overload is characterized by R2* between 130 and 200 s^{-1} and moderate iron overload by R2* between 200 and 320 s^{-1} at 3.0 T, as extrapolated from calibration curves from Wood et al [13]. In this study, two subjects had mild and one had moderate iron overload. As an average iron concentration was found to be relatively low, good results were obtained using MRE with a GRE sequence at 3.0 T. However, it might be appropriate to perform MRE examination at 1.5 T and/or with a spin-echo sequence when available for population with high iron overload incidence.

In a context where the fibrosis stage may lead to enrollment in systematic surveillance programs for hepatocellular carcinoma or to prescription of expensive medication, high accuracy and cost-effectiveness are required for noninvasive techniques. Indeed, there is a need for tools which can accurately distinguish ≤ F1 from ≥ F2, since a significant fibrosis is a major criterion for initiation of long-term treatments such as antiviral B therapy or antifibrotic drugs in HBV and NASH [54]. The significantly higher AUC obtained for detecting stages ≤ F1 from ≥ F2 with MRE compared with that of TE suggests that MRE examinations should preferentially be performed to confirm disease in patients with suspected CLD. A cost-utility analysis of NASH annual noninvasive screening strategies previously showed that MRE was more cost-effective than biopsy [55]. Moreover, accurate staging of F0 from ≥ F1 will be required for early diagnosis and prevention in CLD as early fibrosis is reversible [56, 57]. Significantly higher AUCs obtained for detecting F0 from ≥ F1 with MRE compared with those of TE or pSWE suggest that MRE could also be employed for the early screening of fibrosis. If combined with MRI in the setting of a hepatocellular carcinoma surveillance program, MRE may also have an added value as MRE-determined liver stiffness has been shown to be a significant predictor of hepatocellular carcinoma occurrence in compensated CLD [58].

Multiparametric quantitative MR imaging or ultrasound techniques accounting for the coexistence of inflammation and steatosis will be required to improve fibrosis-staging

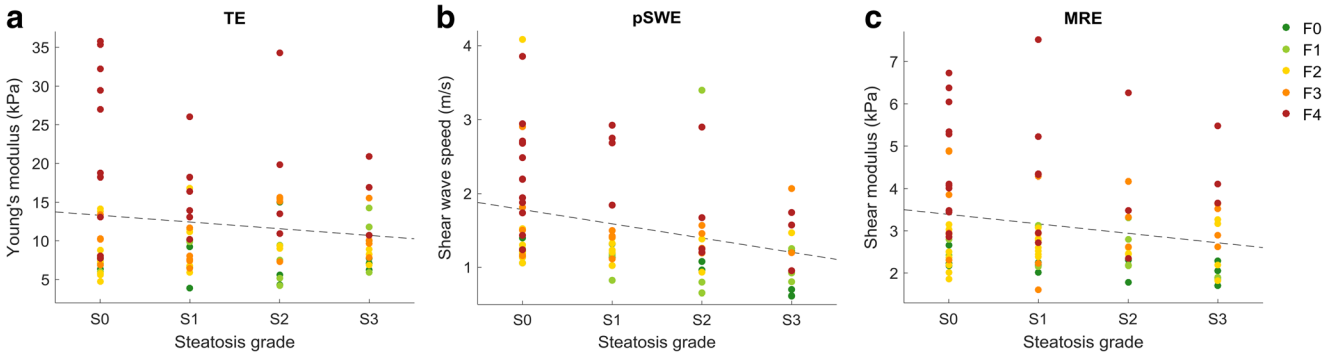

Fig. 6 Scatter plots of stiffness measurements compared with steatosis grades with (**a**) TE, (**b**) pSWE, and (**c**) MRE. Spearman's rho were respectively $\rho = -0.11$ ($p = 0.14$), $\rho = -0.23$ ($p < 0.05$), and $\rho = -0.22$ ($p < 0.05$)

accuracy and further reduce the need for liver biopsy. Tang et al showed that quantitative ultrasound and shear wave elastography provided improved classification accuracy for grading steatosis, inflammation, and fibrosis compared with elastography alone in an animal model [59]. Yin et al proposed a multiparametric quantitative MR imaging model which parameters could accurately predict NAFLD activity score in an animal model [60]. Distinguishing inflammation and steatosis from fibrosis is critical for noninvasive diagnosis and prognosis of CLD with elastography, especially in inflammatory disease and fatty liver disease.

All these endpoints should be achieved with user-friendly screening tools for clinicians sensitive enough to diagnose cirrhotic patients whatever the cause. Future work should include a cost-effectiveness analysis of strategies combining portable ultrasound-based elastographic techniques for point-of-care screening and comprehensive magnetic resonance–based examinations that also permit grading of steatosis, iron, and inflammation [34] in addition to staging of fibrosis in CLD.

In this prospective cross-sectional study, liver stiffness measured by MRE and US-based elastography techniques increased with fibrosis stages and inflammation and decreased with steatosis. MRE provided a diagnostic accuracy higher than US-based elastography techniques for staging of early stages of histology-determined liver fibrosis.

Acknowledgments We thank and acknowledge Mrs. Assia Belblidia, Mrs. Catherine Huet, and Mr. Walid El Abyad for their assistance in patient enrollment and image post-processing. ACUSON S2000 and S3000 ultrasound systems were lent by Siemens Healthineers. Magnetic resonance elastography hardware and software were provided in-kind by Philips Healthcare for this clinical trial.

Funding information This study has received funding by grants from the Canadian Institutes of Health Research (CIHR)-Institute of Nutrition, Metabolism and Diabetes (INMD) (CIHR-INMD #273738 and #301520) and Fonds de recherche du Québec en Santé (FRQS) and Fondation de l'association des radiologistes du Québec (FARQ) Clinical Research Scholarship—Junior 1 and 2 Salary Award (FRQS-FARQ #26993 and #34939) to An Tang. Junior 1 Salary Award from (FRQS #27127) and research salary from McGill University to Giada Sebastiani. Junior 1 Salary Award from FRQS to Marie-Pierre Sylvestre (FRQS #34875).

Compliance with ethical standards

Guarantor The scientific guarantor of this publication is Dr. An Tang.

Conflict of interest The authors of this manuscript declare relationships with the following company: Philips Healthcare Canada (Guillaume Gilbert is an employee of Philips Healthcare Canada).

Statistics and biometry Dr. Marie-Pierre Sylvestre is one of the authors and has significant statistical expertise.

Informed consent Written informed consent was obtained from all subjects in this study.

Ethical approval Institutional Review Board approval was obtained for the two participating institutions, Centre hospitalier de l'Université de Montréal (CHUM) and McGill University Health Centre (MUHC).

Methodology
- prospective
- cross-sectional study
- multicenter study

References

1. Chalasani N, Younossi Z, Lavine JE et al (2012) The diagnosis and management of non-alcoholic fatty liver disease: practice guideline by the American Gastroenterological Association, American Association for the Study of Liver Diseases, and American College of Gastroenterology. Gastroenterology 142:1592–1609
2. Bedossa P, Dargère D, Paradis V (2003) Sampling variability of liver fibrosis in chronic hepatitis C. Hepatology 38:1449–1457
3. Younossi ZM, Loomba R, Anstee QM et al (2017) Diagnostic modalities for non-alcoholic fatty liver disease (NAFLD), non-alcoholic steatohepatitis (NASH) and associated fibrosis. Hepatology. https://doi.org/10.1002/hep.29721
4. Cui J, Ang B, Haufe W et al (2015) Comparative diagnostic accuracy of magnetic resonance elastography vs. eight clinical prediction rules for non-invasive diagnosis of advanced fibrosis in biopsy-proven non-alcoholic fatty liver disease: a prospective study. Aliment Pharmacol Ther 41:1271–1280
5. Xiao G, Zhu S, Xiao X, Yan L, Yang J, Wu G (2017) Comparison of laboratory tests, ultrasound, or magnetic resonance elastography to detect fibrosis in patients with nonalcoholic fatty liver disease: a meta-analysis. Hepatology 66:1486–1501
6. Guo Y, Parthasarathy S, Goyal P, McCarthy RJ, Larson AC, Miller FH (2015) Magnetic resonance elastography and acoustic radiation force impulse for staging hepatic fibrosis: a meta-analysis. Abdom Imaging 40:818–834
7. Xiao H, Shi M, Xie Y, Chi X (2017) Comparison of diagnostic accuracy of magnetic resonance elastography and FibroScan for detecting liver fibrosis in chronic hepatitis B patients: a systematic review and meta-analysis. PLoS One 12:e0186660
8. Myers RP, Pomier-Layrargues G, Kirsch R et al (2012) Feasibility and diagnostic performance of the FibroScan XL probe for liver stiffness measurement in overweight and obese patients. Hepatology 55:199–208
9. Boursier J, Zarski JP, de Ledinghen V et al (2013) Determination of reliability criteria for liver stiffness evaluation by transient elastography. Hepatology 57:1182–1191
10. Dietrich CF, Bamber J, Berzigotti A et al (2017) EFSUMB guidelines and recommendations on the clinical use of liver ultrasound elastography, update 2017 (long version). Ultraschall Med 38:e16–e47
11. Venkatesh SK, Yin M, Ehman RL (2013) Magnetic resonance elastography of liver: technique, analysis, and clinical applications. J Magn Reson Imaging 37:544–555
12. Labranche R, Gilbert G, Cerny M et al (2018) Liver iron quantification with MR imaging: a primer for radiologists. Radiographics 38:392–412
13. Wood JC, Enriquez C, Ghugre N et al (2005) MRI R2 and R2* mapping accurately estimates hepatic iron concentration in transfusion-dependent thalassemia and sickle cell disease patients. Blood 106:1460–1465
14. Obuchowski NA (2005) Estimating and comparing diagnostic tests' accuracy when the gold standard is not binary. Acad Radiol 12:1198–1204

15. Castéra L, Foucher J, Bernard PH et al (2010) Pitfalls of liver stiffness measurement: a 5-year prospective study of 13,369 examinations. Hepatology 51:828–835
16. Woo H, Lee JY, Yoon JH, Kim W, Cho B, Choi BI (2015) Comparison of the reliability of acoustic radiation force impulse imaging and supersonic shear imaging in measurement of liver stiffness. Radiology 277:881–886
17. Friedrich-Rust M, Nierhoff J, Lupsor M et al (2012) Performance of acoustic radiation force impulse imaging for the staging of liver fibrosis: a pooled meta-analysis. J Viral Hepat 19:e212–e219
18. Kim DW, Park C, Yoon HM et al (2019) Technical performance of shear wave elastography for measuring liver stiffness in pediatric and adolescent patients: a systematic review and meta-analysis. Eur Radiol 29:2560–2572
19. Yin M, Glaser KJ, Talwalkar JA, Chen J, Manduca A, Ehman RL (2016) Hepatic MR elastography: clinical performance in a series of 1377 consecutive examinations. Radiology 278:114–124
20. Wagner M, Corcuera-Solano I, Lo G et al (2017) Technical failure of MR elastography examinations of the liver: experience from a large single-center study. Radiology 284:401–412
21. Felker ER, Choi KS, Sung K et al (2018) Liver MR elastography at 3 T: agreement across pulse sequences and effect of liver R2* on image quality. AJR Am J Roentgenol 211:588–594
22. Lee MS, Bae JM, Joo SK et al (2017) Prospective comparison among transient elastography, supersonic shear imaging, and ARFI imaging for predicting fibrosis in nonalcoholic fatty liver disease. PLoS One 12:e0188321
23. Kennedy P, Wagner M, Castéra L et al (2018) Quantitative elastography methods in liver disease: current evidence and future directions. Radiology 286:738–763
24. Singh S, Venkatesh SK, Wang Z et al (2015) Diagnostic performance of magnetic resonance elastography in staging liver fibrosis: a systematic review and meta-analysis of individual participant data. Clin Gastroenterol Hepatol 13:440–451 e446
25. Nierhoff J, Chávez Ortiz AA, Herrmann E, Zeuzem S, Friedrich-Rust M (2013) The efficiency of acoustic radiation force impulse imaging for the staging of liver fibrosis: a meta-analysis. Eur Radiol 23:3040–3053
26. Cui J, Heba E, Hernandez C et al (2016) Magnetic resonance elastography is superior to acoustic radiation force impulse for the diagnosis of fibrosis in patients with biopsy-proven nonalcoholic fatty liver disease: a prospective study. Hepatology 63:453–461
27. Dyvorne HA, Jajamovich GH, Bane O et al (2016) Prospective comparison of magnetic resonance imaging to transient elastography and serum markers for liver fibrosis detection. Liver Int 36:659–666
28. Imajo K, Kessoku T, Honda Y et al (2016) Magnetic resonance imaging more accurately classifies steatosis and fibrosis in patients with nonalcoholic fatty liver disease than transient elastography. Gastroenterology 150:626–637 e627
29. Bohte AE, de Niet A, Jansen L et al (2014) Non-invasive evaluation of liver fibrosis: a comparison of ultrasound-based transient elastography and MR elastography in patients with viral hepatitis B and C. Eur Radiol 24:638–648
30. Friedrich-Rust M, Romen D, Vermehren J et al (2012) Acoustic radiation force impulse-imaging and transient elastography for non-invasive assessment of liver fibrosis and steatosis in NAFLD. Eur J Radiol 81:e325–e331
31. Goertz RS, Zopf Y, Jugl V et al (2010) Measurement of liver elasticity with acoustic radiation force impulse (ARFI) technology: an alternative noninvasive method for staging liver fibrosis in viral hepatitis. Ultraschall Med 31:151–155
32. Rizzo L, Calvaruso V, Cacopardo B et al (2011) Comparison of transient elastography and acoustic radiation force impulse for non-invasive staging of liver fibrosis in patients with chronic hepatitis C. Am J Gastroenterol. https://doi.org/10.1038/ajg.2011.341
33. Iredale JP (2007) Models of liver fibrosis: exploring the dynamic nature of inflammation and repair in a solid organ. J Clin Invest 117:539–548
34. Yin M, Glaser KJ, Manduca A et al (2017) Distinguishing between hepatic inflammation and fibrosis with MR elastography. Radiology 284:694–705
35. Salameh N, Larrat B, Abarca-Quinones J et al (2009) Early detection of steatohepatitis in fatty rat liver by using MR elastography. Radiology. https://doi.org/10.1148/radiol.2523081817
36. Chen J, Talwalkar JA, Yin M, Glaser KJ, Sanderson SO, Ehman RL (2011) Early detection of nonalcoholic steatohepatitis in patients with nonalcoholic fatty liver disease by using MR elastography. Radiology 259:749–756
37. Hartl J, Denzer U, Ehlken H et al (2016) Transient elastography in autoimmune hepatitis: timing determines the impact of inflammation and fibrosis. J Hepatol 65:769–775
38. Shi Y, Guo Q, Xia F et al (2014) MR elastography for the assessment of hepatic fibrosis in patients with chronic hepatitis B infection: does histologic necroinflammation influence the measurement of hepatic stiffness? Radiology 273:88–98
39. Yoneda M, Suzuki K, Kato S et al (2010) Nonalcoholic fatty liver disease: US-based acoustic radiation force impulse elastography. Radiology 256:640–647
40. Yanrong Guo, Haoming Lin, Xinyu Zhang, Huiying Wen, Siping Chen, Xin Chen (2017) The influence of hepatic steatosis on the evaluation of fibrosis with non-alcoholic fatty liver disease by acoustic radiation force impulse. Conf Proc IEEE Eng Med Biol Soc 2017:2988–2991
41. Petta S, Maida M, Macaluso FS et al (2015) The severity of steatosis influences liver stiffness measurement in patients with nonalcoholic fatty liver disease. Hepatology 62:1101–1110
42. Yin M, Talwalkar JA, Glaser KJ et al (2007) Assessment of hepatic fibrosis with magnetic resonance elastography. Clin Gastroenterol Hepatol 5:1207–1213 e1202
43. Venkatesh SK, Wang G, Teo LL, Ang BW (2014) Magnetic resonance elastography of liver in healthy Asians: normal liver stiffness quantification and reproducibility assessment. J Magn Reson Imaging 39:1–8
44. Kazemirad S, Zhang E, Nguyen BN et al (2016) Detection of steatohepatitis in a rat model by using spectroscopic shear-wave US elastography. Radiology. https://doi.org/10.1148/radiol.2016160308:160308
45. Tang A, Desai A, Hamilton G et al (2015) Accuracy of MR imaging-estimated proton density fat fraction for classification of dichotomized histologic steatosis grades in nonalcoholic fatty liver disease. Radiology 274:416–425
46. Yokoo T, Serai SD, Pirasteh A et al (2018) Linearity, bias, and precision of hepatic proton density fat fraction measurements by using MR imaging: a meta-analysis. Radiology 286:486–498
47. Karlas T, Petroff D, Sasso M et al (2017) Individual patient data meta-analysis of controlled attenuation parameter (CAP) technology for assessing steatosis. J Hepatol 66:1022–1030
48. Caussy C, Alquiraish MH, Nguyen P et al (2018) Optimal threshold of controlled attenuation parameter with MRI-PDFF as the gold standard for the detection of hepatic steatosis. Hepatology 67:1348–1359
49. Friedrich-Rust M, Ong MF, Martens S et al (2008) Performance of transient elastography for the staging of liver fibrosis: a meta-analysis. Gastroenterology 134:960–974
50. Shin HJ, Kim MJ, Kim HY, Roh YH, Lee MJ (2016) Comparison of shear wave velocities on ultrasound elastography between different machines, transducers, and acquisition depths: a phantom study. Eur Radiol 26:3361–3367
51. Yoshimitsu K, Mitsufuji T, Shinagawa Y et al (2016) MR elastography of the liver at 3.0 T in diagnosing liver fibrosis grades; preliminary clinical experience. Eur Radiol 26:656–663

52. Park HS, Kim YJ, Yu MH, Choe WH, Jung SI, Jeon HJ (2014) Three-tesla magnetic resonance elastography for hepatic fibrosis: comparison with diffusion-weighted imaging and gadoxetic acid-enhanced magnetic resonance imaging. World J Gastroenterol 20: 17558–17567
53. Wang J, Glaser KJ, Zhang T et al (2018) Assessment of advanced hepatic MR elastography methods for susceptibility artifact suppression in clinical patients. J Magn Reson Imaging 47:976–987
54. Zou X, Zhu MY, Yu DM et al (2017) Serum WFA(+) -M2BP levels for evaluation of early stages of liver fibrosis in patients with chronic hepatitis B virus infection. Liver Int 37:35–44
55. Zhang E, Wartelle-Bladou C, Lepanto L, Lachaine J, Cloutier G, Tang A (2015) Cost-utility analysis of nonalcoholic steatohepatitis screening. Eur Radiol 25:3282–3294
56. Zhao J, Zhai F, Cheng J et al (2017) Evaluating the significance of viscoelasticity in diagnosing early-stage liver fibrosis with transient elastography. PLoS One 12:e0170073
57. Ellis EL, Mann DA (2012) Clinical evidence for the regression of liver fibrosis. J Hepatol 56:1171–1180
58. Lee DH, Lee JM, Chang W et al (2018) Prognostic role of liver stiffness measurements using magnetic resonance elastography in patients with compensated chronic liver disease. Eur Radiol 28: 3513–3521
59. Tang A, Destrempes F, Kazemirad S, Garcia-Duitama J, Nguyen BN, Cloutier G (2019) Quantitative ultrasound and machine learning for assessment of steatohepatitis in a rat model. Eur Radiol 29: 2175–2184
60. Yin Z, Murphy MC, Li J et al (2019) Prediction of nonalcoholic fatty liver disease (NAFLD) activity score (NAS) with multiparametric hepatic magnetic resonance imaging and elastography. Eur Radiol. https://doi.org/10.1007/s00330-019-06076-0